

Diagnostic Evaluation of NuMI Hadron Monitor Ion Chambers

Bernadette Haig
Fordham University

Katsuya Yonehara
Fermi National Accelerator Laboratory
 (Dated: August 17, 2017)

The performance of the NuMI Hadron Monitor ion chambers was evaluated. Possible sources of ion chamber performance degradation are discussed, based upon analysis of Monitor data. The quality of the signal is reviewed, and it is concluded that the Monitor still functions for its main tasks. Repair is not possible, but replacement of the Hadron Monitor during the 2017 summer shutdown was not deemed necessary. Lastly, a diagnostic apparatus for potential impurity of the helium gas inside the chamber has been designed and installed. A vacuum chamber is connected to the Hadron Monitor exhaust line to collect gas samples. These samples are analyzed by a GCMS (gas chromatograph-mass spectrometer).

I. INTRODUCTION

The Hadron Monitor sits in the NuMI beamline at Fermilab, between the end of the Decay Pipe and the Absorber, and measures the spatial distribution of un-interacted protons and undecayed pions.[1] The current Hadron Monitor has been in operation since fall 2013. The major tasks of the Hadron Monitor include alignment of the primary proton beam on the target, tracking the center position of the beam during normal beam operation, and monitoring the target's long-term deterioration.[1] Unfortunately, the current Hadron Monitor is not useful for this last task, since some pixels are malfunctioning. The central pixel is the most important for performing the first two tasks. We discuss several hypotheses pertaining to the declining performance of the Hadron Monitor based upon our analysis of past Monitor data; we also present a design for a diagnostic system to confirm one of these hypotheses, and some preliminary results.

high-purity helium gas (99.9995%). Each pixel consists of a single ion chamber with a pair of ceramic plates, spaced 1 mm apart.[1] The beam passes through the Monitor, perpendicular to the pixel matrix, and ionizes the helium gas inside. In each pixel, a power supply generates a positive potential to one plate to collect the electrons produced, while the negatively charged plate collects the positive ions. The accumulated positive charges are fed into an integrator, which converts them into a beam signal. A block diagram of one ion chamber and peripheral electric circuit is shown in Fig. 1. A large capacitor is connected upstream and downstream of the plates to hold a bias voltage in the plate gap. This capacitance and impedance are $5 \mu\text{F}$ and $100 \text{ k}\Omega$, respectively.

The configuration of the Hadron Monitor's pixels is shown in Fig. 2. Pixel #176 (yellow) is the central pixel. In order to evaluate the horizontal beam profile, we analyzed the signal from #173 to #179 (light blue belt). For the vertical profile, we analyzed every seventh pixel from #155 to #197 (light green belt).

II. APPARATUS

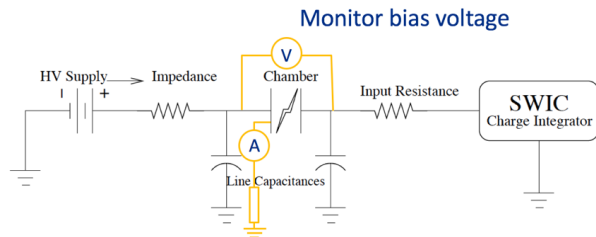


FIG. 1. Block diagram of a Hadron Monitor ion chamber and peripheral electric circuit.

The Hadron Monitor is approximately one meter high by one meter wide, and is comprised of 49 pixels, seven on a side. The pixels sit inside an aluminum box filled with

152	153	154	155	156	157	158
159	160	161	162	163	164	165
166	167	168	169	170	171	172
173	174	175	176	177	178	179
180	181	182	183	184	185	186
187	188	189	190	191	192	193
194	195	196	197	198	199	104

FIG. 2. Hadron Monitor pixel configuration

III. PERFORMANCE ANALYSIS

A. Ion Chamber Signal

Fig. 3 shows snapshots of the Hadron Monitor signal taken in October 2013 and May 2017. The Hadron Monitor was new in October 2013. After almost four years' operation, several pixels are malfunctioning, as shown by the blue pads in the May 2017 data. (Note the change in scale between the two charts.)

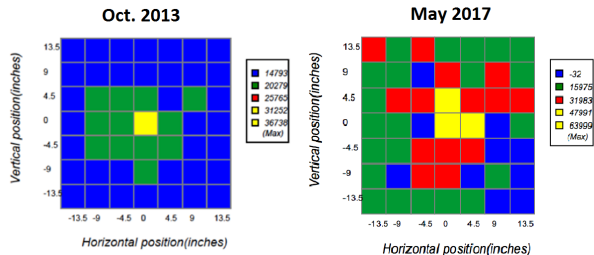


FIG. 3. Hadron Monitor signal, Oct. 2013 and May 2017.

Fig. 4 shows the vertical and horizontal cross-sectional beam profiles taken in October 2013 (blue) and May 2017 (red). The green dashed line represents the beam profile (simulated in G4beamline) when the horn is turned off. The observed beam profile in October 2013 is symmetric and has a long tail. It is known that the central distribution is dominated by elastically scattered protons and that the long tail in the measurement consists of particles focused by the horn. These are not clearly shown in the May 2017 data. #175 and #178 show very low signal in 2017. These pixels are malfunctioning.

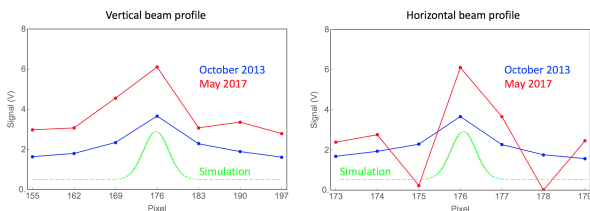


FIG. 4. Vertical and horizontal beam profiles, Oct. 2013 and May 2017.

B. Beam Signal Linearity

$$\text{signal} = V_{\text{beam on}} - V_{\text{beam off}}$$

$$\text{gain} = \frac{V_{\text{beam on}} - V_{\text{beam off}}}{I_{\text{beam}}}$$

$$\text{linearity} = \frac{\text{signal}}{I_{\text{beam}}}$$

The linearity of the beam signal is calculated as the gain, by subtracting the pedestal from the applied bias voltage to get the beam signal and dividing this by the beam current.

It is critical to consider beam size when analyzing signal linearity as a function of beam intensity because the Hadron Monitor is very sensitive to the beam size. This sensitivity is due to the fact that some amount of primary protons which distribute at the tail miss the target and directly hit the Hadron Monitor. The wider the beam, the greater the number of protons that miss the target.

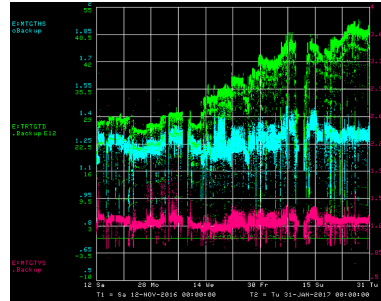


FIG. 5. Beam intensity and vertical and horizontal beam profiles, central pixel, Nov. 2016 - Jun. 2017.

Fig. 5 was taken from pixel #176; it shows constant vertical and horizontal beam profiles (blue and pink), reflecting consistent beam size, as beam intensity (green) is increased from November 2016 to January 2017. In this time span, the beam intensity was changed significantly, but the beam size was held relatively constant, which makes data taken during this period ideal for analyzing signal linearity as a function of beam intensity.

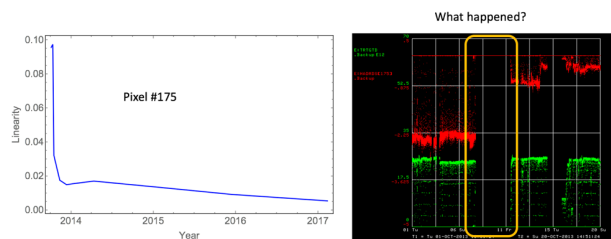


FIG. 6. Beam signal linearity on #175 as a function of operation time.

Pixel #175 began to malfunction almost immediately after installation— within a month of operation. Fig. 6 shows the linearity change on #175 as a function of operation time. The output signal dropped sharply, only a few days after the NuMI beam start running. Something happened between 8 and 11 October 2013, when the beam was stopped.

The functionality of pixel #178 declined gradually, but also eventually experienced a sudden drop in signal, as shown in Fig. 7. #178 responded predictably to beam intensity until October 2015. It stopped temporarily between October 2015 and April 2016, during an increase

in beam intensity. The signal returned after this time, but again disappeared during another increase in beam intensity in April 2017. Since that time, there has been no further response from #178.

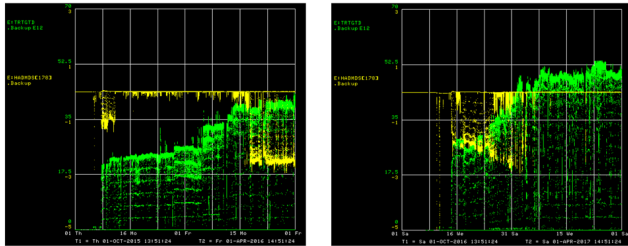


FIG. 7. Beam intensity from Oct. 2015 - Apr. 2016, Oct. 2016 - Apr. 2017 (green); pixel #178 response (yellow).

Fig. 8a shows the observed linearity as a function of the primary beam intensity. The gain is reduced from 0.17 to 0.13 when the beam intensity increases from 26 to 50 e12 ppp (protons per pulse). The dashed lines show fitting curves for pixel #176 beam response, using different functions. The resulting curves are very similar to a past ion chamber test measurement taken in He, as shown in Fig. 8b. The similarity of the central pixel data to the test data from a functional ion chamber seems to indicate that relatively good beam signal linearity is maintained in this pixel; however, there is still some loss.

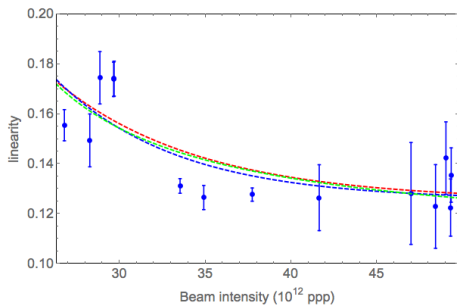


FIG. 8a. Observed beam signal linearity on #176 as a function of primary beam intensity.

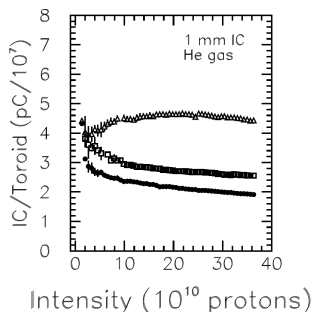


FIG. 8b. Ion chamber test measurement taken in He, prior to Hadron Monitor installation.

IV. POTENTIAL LOSS SOURCES

Here, we discuss several possible sources of beam signal loss, according to our analysis of Hadron Monitor data from October 2013 to May 2017.

A. Electrical Malfunction

The decline of pixels #175 and #178, although not identical, show similarities, suggesting that they might be attributed to the same cause. #175 died suddenly, after a short amount of time. #178 experienced a slow malfunction (perhaps due to radiation damage), but then dropped off suddenly in a fashion similar to that of #175. This sudden failure seems to indicate an electrical problem.

B. Leakage Current

Ideally, there should be no leakage current on the ion chamber plates, since they are electrically isolated from the ground; however, in practice, a leakage current has been observed by a current monitor on the power supply. This indicates that the plates weakly short to the ground. The resistance of this shortage is on the order of M Ω or higher, based upon the observed bias voltage (40-100 V) and leakage current (a few nA to 100 μ A). The shortage changes the bias voltage on the plates and affects the stability and linearity of the output signal.

A pedestal in the ion chamber signal represents a conductivity in the plate gaps when the beam is turned off ($V_{beam\ off}$). The observed pedestal varies slightly, but remains small in all pixels studied, at all times. There does not appear to be a size correlation between the observed leakage current and pedestal. This suggests that the charge conduction in the plate gap is not the source of the leakage current; the true source is unknown.

C. Space Charge Effect

Space charge is another potential source of linearity loss in the beam signal. A strong space charge effect is capable of significantly increasing the number of ionized electrons in an ion chamber. A detailed investigation was made for an ion chamber in numerical simulation, and by using a test beam before installation. Fig. 9 shows the observed ion chamber signal as a function of the bias voltage, produced with a test beam.

This test suggests that the linearity of the output signal can fluctuate by $\sim 10\%$ when the bias voltage is altered ± 20 V at 100 V, while the ion chamber accepts $22e12$ particles. Additionally, we found that between November 2016 and January 2017 (when the beam intensity was increased without changing the beam size),

the linearity dropped by about 30%, when the beam intensity increased by 50%.

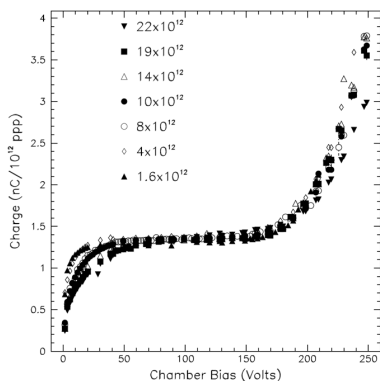


FIG. 9. Ion chamber signal as a function of space charge, as measured by a test beam.

D. Gas Impurity

The loss of linearity observed on the central pixel of the Hadron Monitor may be caused by impurity of the He gas inside the Hadron Monitor. (This impurity is another potential cause of #178's slow decline before its sudden death.)

An electronegative gas, like O_2 , captures ionized electrons and drastically changes the plasma dynamic. Fig. 10 shows a block diagram of the gas regulation system. Unlike the Muon Monitors, the Hadron Monitor does not have a bubbler to prevent backflow of gas in the exhaust line—only a long pigtail of tubing to create a high gas-flow impedance. It is suspected that air is leaking back into the Hadron Monitor through this line and contaminating the He gas inside.

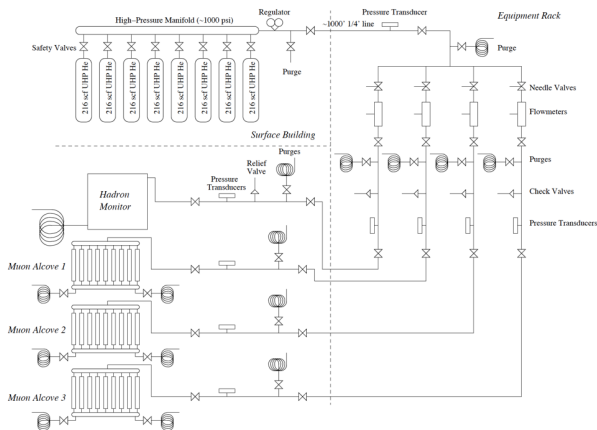


FIG. 10. Block diagram of gas regulation system.

One possible way to reduce the likelihood of backflow is to increase the gas flow rate. This minimizes the O_2

level; however, the Hadron Monitor is not very sturdy, and overpressurizing the chamber warps it, and opens another leakage path. Fig. 11 shows the observed O_2 level in the chamber as a function of the gas flow rate, measured with an Illinois Instruments Oxygen Analyzer when the Hadron Monitor was first installed.

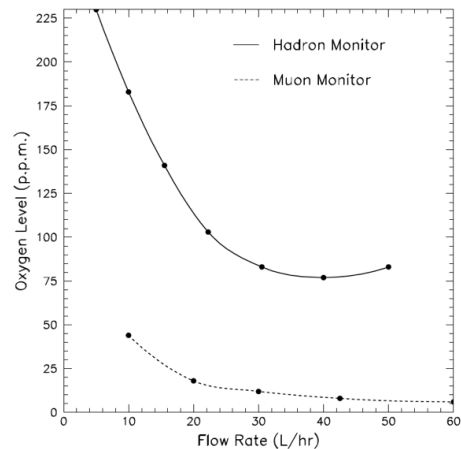


FIG. 11. Observed O_2 level in ion chamber.

V. DIAGNOSTIC SYSTEM

The Hadron Monitor is not designed to be taken apart; currently, no means exists of repairing damaged pixels without replacing the entire Monitor. However, possible He impurity due to backflow in the chamber's exhaust line is more easily addressed. A small vacuum chamber has been designed, manufactured, and installed in the Absorber Hall to collect exhaust gas from the Hadron Monitor. Fig. 12 shows a schematic of this sample chamber, connected to the Hadron Monitor's exhaust line.

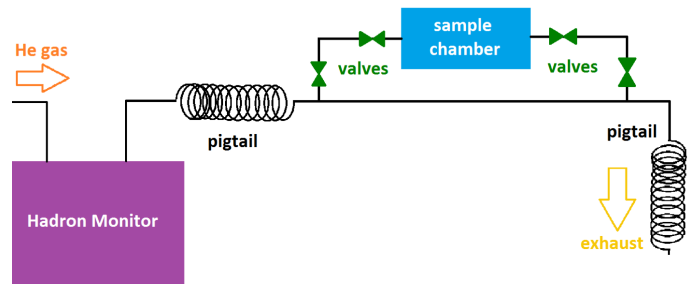


FIG. 12. Diagram showing sample chamber connected to Hadron Monitor exhaust line.

The exhaust line was extended from the end of the existing pigtail, and another 50' pigtail was created. A bypass line containing the sample chamber and four ball valves was added, with two stainless steel tee fittings. To collect the exhaust gas, the bypass line valves were left open over a period of several days. The sample chamber

was then removed by closing all four valves and disconnecting the chamber from the bypass line. The two valves proximal to the chamber held the gas inside; the two distal valves prevented air leakage back into the exhaust tube from the open bypass line.

We brought the sample chamber to the C0 building where a GCMS (gas chromatograph-mass spectrometer) is housed. To extract the gas from the sample chamber, we connected it to a small piece of tubing, another ball valve, and a vacuum pump, as shown in Fig. 13. The distal ball valve was opened, and all of the tubing was pumped down. Then we closed the distal valve and opened the proximal valve, allowing the gas from the chamber to flow into the small piece of tubing. The proximal valve was then closed, and the gas was sampled from the small piece of tubing using a gas-tight syringe, and then injected into a port on the GCMS.



FIG. 13. Tubing being pumped down to allow for gas sampling from chamber with gas-tight syringe. After sampling, the gas is injected into a GCMS to discern the degree of contamination in the Hadron Monitor's He environment.

VI. PRELIMINARY RESULTS

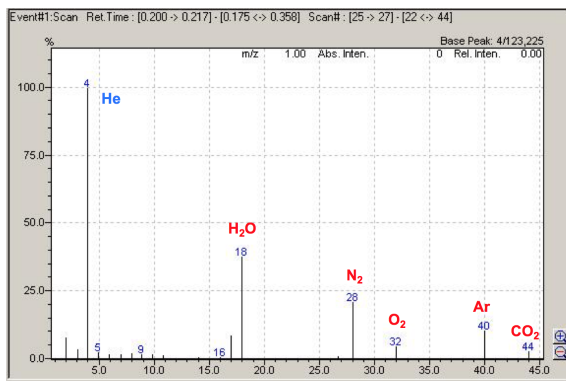


FIG. 14. Qualitative spectrum of gas sample produced by GCMS. A high He peak is observed, as well as relatively high intensities of contaminant gas.

Fig. 14 shows preliminary qualitative results produced by the GCMS. The highest intensity peak is found at an

atomic mass of 4 (He) with shorter peaks at 18 (H_2O), 28 (N_2), 32 (O_2), 40 (Ar), and 44 (CO_2). These results appear to be in agreement with our hypothesis of atmospheric contamination inside the Hadron Monitor; however, we did not expect to see a helium peak, since the carrier gas used in the GCMS is also helium. This abnormality casts doubt on the measurement.

VII. FUTURE WORK

The GCMS measurements must be repeated with new samples to ascertain their validity. Additionally, it would be helpful to convert the qualitative readings that were produced into concentrations, to determine the exact degree of He contamination inside the Hadron Monitor. This might be facilitated by using an RGA (residual gas analyzer) instead of a GCMS. It might also be beneficial to explore more direct ways of measuring the gas; this could eliminate the possibility of leakage into the sample chamber from the air, between the removal of the chamber from the Absorber Hall and the testing of the gas in the GCMS. An oxygen analyzer is considered for this purpose.

VIII. CONCLUSION

The performance of the NuMI Hadron Monitor was evaluated by analyzing measurements taken since October 2013. Several pixels near the center are malfunctioning, but there is no means of individually repairing or replacing them. The central pixel itself has experienced some loss of beam signal linearity, but still matches initial ion chamber test measurements fairly well. We have determined that its performance is reliable enough to execute the primary tasks of the Hadron Monitor, which rely most heavily on this central pixel. Therefore, it is not yet necessary to replace the Monitor.

Additionally, we have designed an apparatus to conclusively diagnose a possible contamination of the helium gas inside the Hadron Monitor. The gas being vented from the Hadron Monitor's exhaust line is collected into a small chamber, so that it may be injected into a GCMS (gas chromatograph-mass spectrometer) to determine its composition. Preliminary results seem to indicate that atmospheric contamination is present, but these measurements must be repeated before they can be considered reliable.

ACKNOWLEDGMENTS

We would like to acknowledge Bob Zwaska's informed advice throughout this project, as well as the use of several figures from his doctoral thesis. We also thank Chris Kelly, Kris Anderson, and members of the Target Systems Department who lent their expertise and helpful

feedback, and Anna Pla-Dalmau for her guidance on the use of the GCMS. BH gratefully acknowledges the mentorship of Katsuya Yonehara, Donovan Tooke and Dave Peterson, as well as the support of Elliott McCrory, San-

dra Charles, and everyone else at SIST.

Work supported by Fermilab Research Alliance, LLC under Contract No. DE-AC02-07CH11359.

- [1] Robert M. Zwaska, “Accelerator Systems and Instrumentation for the NuMI Neutrino Beam.” FERMILAB-THESIS-2005-73. Dec 2005.

LIST OF FIGURES

1	Block diagram of a Hadron Monitor ion chamber and peripheral electric circuit.	1	8a	Observed beam signal linearity on #176 as a function of primary beam intensity.	3
2	Hadron Monitor pixel configuration	1	8b	Ion chamber test measurement taken in He, prior to Hadron Monitor installation.	3
3	Hadron Monitor signal, Oct. 2013 and May 2017.	2	9	Ion chamber signal as a function of space charge, as measured by a test beam.	4
4	Vertical and horizontal beam profiles, Oct. 2013 and May 2017.	2	10	Block diagram of gas regulation system.	4
5	Beam intensity and vertical and horizontal beam profiles, central pixel, Nov. 2016 - Jun. 2017.	2	11	Observed O ₂ level in ion chamber.	4
6	Beam signal linearity on #175 as a function of operation time.	2	12	Diagram showing sample chamber connected to Hadron Monitor exhaust line.	4
7	Beam intensity from Oct. 2015 - Apr. 2016, Oct. 2016 - Apr. 2017 (green); pixel #178 response (yellow).	3	13	Tubing being pumped down to allow for gas sampling from chamber with gas-tight syringe. After sampling, the gas is injected into a GCMS to discern the degree of contamination in the Hadron Monitor’s He environment.	5
			14	Qualitative spectrum of gas sample produced by GCMS. A high He peak is observed, as well as relatively high intensities of contaminant gas.	5